

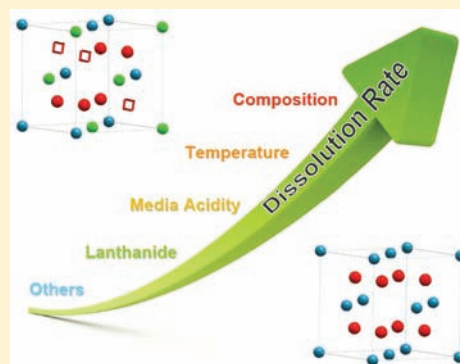
Dissolution of Cerium(IV)–Lanthanide(III) Oxides: Comparative Effect of Chemical Composition, Temperature, and Acidity

D. Horlait, N. Clavier,* S. Szenknect, N. Dacheux, and V. Dubois

ICSM, UMR 5257 CEA/CNRS/UM2/ENSCM, Site de Marcoule–Bât. 426, BP 17171, 30207 Bagnols/Cèze, Cedex, France

Supporting Information

ABSTRACT: The dissolution of $Ce_{1-x}Ln_xO_{2-x/2}$ solid solutions was undertaken in various acid media in order to evaluate the effects of several physicochemical parameters such as chemical composition, temperature, and acidity on the reaction kinetics. The normalized dissolution rates ($R_{L,0}$) were found to be strongly modified by the trivalent lanthanide incorporation rate, due to the presence of oxygen vacancies decreasing the samples cohesion. Conversely, the nature of the trivalent cation considered only weakly impacted the $R_{L,0}$ values. The dependence of the normalized dissolution rates on the temperature then appeared to be of the same order of magnitude than that of chemical composition. Moreover, it allowed determining the corresponding activation energy ($E_A \approx 60\text{--}85 \text{ kJ}\cdot\text{mol}^{-1}$) which accounts for a dissolution driven by surface-controlled reactions. A similar conclusion was made regarding the acidity of the solution: the partial order related to (H_3O^+) reaching about 0.7. Finally, the prevailing effect of the incorporation of aliovalent cations in the fluorite-type CeO_2 matrix on the dissolution kinetics precluded the observation of slight effects such as those linked to the complexing agents or to the crystal structure of the samples.



1. INTRODUCTION

Mixed actinides dioxides such as $(U,Pu)O_2$ (MO_x) are currently employed in Pressurized Water nuclear Reactors (PWR) nuclear reactors and are expected to be the reference fuels for several concepts of Gen III and Gen IV reactors.^{1,2} Moreover, the development of rapid neutrons reactors could allow operating the recycling of minor actinides such as neptunium, americium, or curium, directly inside the reactor core, or in UO_2 -based fertile blankets located all around the core.³ In this latter scenario, it was already demonstrated that americium should be mainly present in the trivalent oxidation state.^{4,5} Also, several concepts plan to incorporate trivalent lanthanides such as gadolinium or erbium inside fuel elements to act as neutron absorbers.⁶ In both cases, the effect of the trivalent element incorporation in the fluorite-type UO_2 matrix on its physicochemical properties should be evaluated to anticipate and optimize properly the life-cycle of the fuel. Particularly, the chemical durability of such compounds must be evaluated in order to operate their reprocessing (quantitative dissolution in acidic media) or their direct storage in deep geological environment (leaching of the fuel by groundwater).

In this context, multiparametric studies that evidenced the effects of temperature, acidity, composition^{7–9} or, more recently, microstructural parameters,^{10–13} on the dissolution rates of various AnO_2 oxides were already reported in the literature. Nevertheless, very few of them dealt with the incorporation of trivalent elements in the structure and the potential consequences linked to the formation of punctual defects in the fluorite-type matrix. Indeed, the incorporation of trivalent elements, such as lanthanides, in MO_2 structures ($M =$

Th, U, Ce) was systematically found to occur with the formation of oxygen vacancies that counterbalance the charge deficit.^{14–19} Consequently, one can expect a variation of the energy of cohesion of the structure leading to a significant variation in its chemical durability.²⁰

As such effect was already observed when incorporating small amounts of neodymium in the CeO_2 structure,¹² this paper is thus devoted to a first study of $M^{IV}_{1-x}Ln_xO_{2-x/2}$ compounds on a full range of composition (including various incorporation rate and doping elements) through the preparation and the dissolution of $Ce_{1-x}Ln_xO_{2-x/2}$ solid solutions in nitric media. Indeed, $Ce^{IV}O_2$ crystallizes in the same structure than $Pu^{IV}O_2$ and $U^{IV}O_2$ (fluorite, $Fm\bar{3}m$ space group: JCPDS file nos. 01-081-0792,²¹ 00-051-0798,²² and 01-073-2293,²³ for CeO_2 , PuO_2 , and UO_2 , respectively) and Ce^{4+} ion presents a close ionic radius compared to plutonium whatever the coordination considered.²⁴ Similarly, lanthanide sesquioxides ($Ln^{III}_2O_3$) are usually considered as nonradioactive surrogates for actinide sesquioxides ($An^{III}_2O_3$) such as Am_2O_3 and Cm_2O_3 .^{4,5}

In order to compare the relative effects of well-known parameters with that of composition, a multiparametric study involving temperature, acidity, lanthanide incorporation rate, and trivalent lanthanide nature was then set up to prioritize the parameters impacting the initial normalized dissolution rates of $Ce_{1-x}Ln_xO_{2-x/2}$ mixed oxides.

Received: January 12, 2012

Published: February 29, 2012

2. EXPERIMENTAL SECTION

2.1. Synthesis and Characterization. Ceria-based mixed oxides were prepared through a two-step procedure composed by the initial oxalic coprecipitation of the cations followed by a heat treatment at 1000 °C as detailed in previously published work.¹⁹ For all the samples, the precise chemical composition was determined through statistical X-EDS measurements (based on at least 20 data points) conducted on a FEI QUANTA 200 ESEM FEG microscope: on the basis of the results dispersion, an absolute accuracy of ± 0.01 on the average value was assumed (Table 1).

Table 1. Chemical Composition, Crystal Structure, and Specific Surface Area (S_{SA}) of the $Ce_{1-x}Ln_xO_{2-x/2}$ Samples Prepared through Oxalic Coprecipitation^a

Ln ^{III}	x_{Ln} (X-EDS)	structure	S_{SA} ($m^2 \cdot g^{-1}$)	Ln ^{III}	x_{Ln} (X-EDS)	structure	S_{SA} ($m^2 \cdot g^{-1}$)
La	0.00	F	1.8	Eu	0.61	C	5.4
	0.28	F	8.1		0.26	F	3.3
	0.58	F	4.0		0.64	C	2.9
Nd	0.10	F	4.7	Dy	0.28	F	2.5
	0.20	F	4.9		0.62	C	2.3
	0.24	F	5.4	Er	0.12	F	1.3
	0.29	F	3.5		0.15	F	1.1
	0.34	F	4.0	0.20	F	3.3	
	0.39	F	5.2	0.25	F	2.6	
	0.42	C	4.1	0.34	F	0.8	
	0.48	C	3.1	0.39	C	3.6	
	0.59	C	4.1	0.51	C	1.5	
	0.68	C	2.8	0.59	C	2.6	
	0.73	C	3.8	0.75	C	4.0	
0.74	A + C	3.7	0.80	C	2.5		
0.79	A + C	2.9	0.90	C	3.5		
Sm	0.90	A + C	5.4	Yb	0.29	F	1.9
	0.97	A + C	5.1		0.60	C + C	3.2
	0.62	C	2.8				

^aF stands for fluorite, C, for the $Ia\bar{3}$ cubic superstructure (bixbyite), and A, for the hexagonal form of Ln_2O_3 sesquioxides.

From XRD characterization (Bruker D8 Advance X-ray diffractometer using $Cu K\alpha_{1,2}$ radiation, $\lambda = 1.5418 \text{ \AA}$), the obtained samples were found to present different crystal structures depending on the trivalent rare earth element considered and its incorporation rate. In the case of the $Ce_{1-x}Nd_xO_{2-x/2}$ series, the original fluorite structure of CeO_2 was maintained up to $x_{Nd} \approx 0.4$. For $0.42 < x_{Nd} < 0.74$, the formation of a cubic superstructure (bixbyite, space group $Ia\bar{3}$) was noted, while the formation of additional Nd_2O_3 (hexagonal, space group $P\bar{3}1m$) was observed when reaching the incorporation limit ($x_{Nd} > 0.73$).

Finally, specific area measurements were carried out using the BET method (N_2 adsorption at 77 K) for normalization purposes either with a Micromeritics TRISTAR or a Micromeritics ASAP 2020 device. All the results related to the characterization of the various powdered samples prepared are gathered in Table 1.

2.2. Dissolution Experiments. All the acidic solutions used for the dissolution tests (HNO_3 , HCl , and H_2SO_4) were prepared from analytical grade reagents (supplied by Sigma or Fisher).

A 29 mL portion of acidic solution was introduced into sealed polytetrafluoroethylene (PTFE) containers (from Saville) and contacted with about 200 mg of powdered sample. For 10^{-4} – 10^{-2} M HNO_3 media, 0.1 M KNO_3 was also added to maintain the ionic strength of the leaching media.

The dissolution of the solid was then monitored through regular uptakes of the leachate then inductively coupled plasma atomic emission spectrometry (ICP-AES) measurements of elementary

concentrations. Given the wide range of dissolution rates expected, three different protocols were used in order to optimize the accuracy of the measurements:

- For the slowest dissolution rates expected, the samples were usually placed into an oven between 40 and 90 °C, or into melting ice ($T \approx 2 \text{ °C}$), without any stirring. For each sampling, 1.1 mL of the leaching solution was uptaken and centrifuged at 12 000 rpm. In such conditions, the fractionation limit allowed avoiding the presence of particles or colloids approximately bigger than 10 nm.²⁵ Then 1 mL of the solution was introduced in 9 mL of deionized water before ICP-AES measurements, resulting in a dilution factor of 10. In order to maintain the leachate volume, fresh solution was finally added in the reactor.
- When the complete dissolution of the samples was expected to be reached within a week, the solutions were continually blended using a magnetic stirring bar. For every sampling, 200 μL of the leachate were removed, diluted with 300 μL of deionized water, and then centrifuged at 12 000 rpm. Finally, 200 μL of solution was placed in 9.8 mL of deionized water (dilution factor of 125).
- When the complete dissolution of the powdered sample was expected to occur within a few minutes, it appeared impossible to follow the concentrations in solution with a good accuracy. The dissolution rate was thus evaluated through the time required for the total disappearance of the solid phase in the container. In such conditions, the relative uncertainty associated to the $R_{L,0}$ value was evaluated to be around $\pm 50\%$.

The concentrations of the elements released in the solution were determined by ICP-AES using a Spectro Arcos EOP apparatus. In this purpose, the spectrometer was calibrated with SPEX standard solutions. The emission bands considered for each lanthanide element are detailed in the Supporting Information.

2.3. Determination of the Normalized Dissolution Rates. The normalized weight losses (N_L , also called normalized leachings and expressed in grams per square meter) were calculated from the elementary concentrations after normalization by the reactive surface S (m^2) of the sample in contact with the solution and by the mass ratio of the element considered in the solid (f_i , expressed as the ratio between the mass of the considered element and the overall mass of the sample),²⁶ following the equation:

$$N_L(i) = \frac{m_i}{f_i S} = \frac{C_i V M_i}{f_i S} \quad (1)$$

where m_i (g) corresponds to the total amount of the element i measured in the solution; C_i is the concentration of the lanthanide element in the leachate ($\text{mol} \cdot \text{L}^{-1}$); V is the volume of leachate (L); M_i is the molar mass of the element considered in the solid ($\text{g} \cdot \text{mol}^{-1}$).

Deriving eq 1 as a function of leaching time led to the normalized dissolution rate of the element i ($R_L(i)$, $\text{g} \cdot \text{m}^{-2} \cdot \text{d}^{-1}$) as follows:²⁷

$$R_L(i) = \frac{dN_L(i)}{dt} = \frac{1}{f_i S} \frac{dm_i}{dt} \approx \frac{VM_i}{f_i S} \frac{dC_i}{dt} \quad (2)$$

In this study, M_i and S were supposed to remain constant during the dissolution. Thereafter, the reaction of dissolution was called to be stoichiometric if all the elements i were released in the leachate with the same normalized dissolution rates. Conversely, if one element was released more rapidly from the solid (e.g., like fluorine in the britholite structure²⁸), the dissolution was called to be selective regarding to the considered element. Moreover, the dissolution was qualified as congruent when all the normalized dissolution rates were close ($1/3 < R_i/R_j < 3$), i.e. when all the elements were released with the same ratios than the stoichiometry of the initial material.^{29,30} In the opposite, it was called to be incongruent if at least one element was precipitated as neoformed phases in the back end of the initial reaction of dissolution. It is also obviously the case if the dissolution is initially selective regarding the elements constituting the solid.

2.4. Influence of Acidity and Temperature on the R_L Values. Many authors demonstrated the role of acidity and temperature on the

behavior of the materials during dissolution. For a large variety of minerals,^{7–9,12,13,31–39} the dependence of the normalized dissolution rate R_L with the proton activity (for $\text{pH} < 7$) and with temperature was described by the following equation:

$$R_L = k'_T(\text{H}_3\text{O}^+)^n = k'_T(\gamma_{\text{H}_3\text{O}^+}[\text{H}_3\text{O}^+])^n = k''(\text{H}_3\text{O}^+)^n e^{-E_A/RT} \quad (3)$$

In this expression, R_L refers to the proton-promoted normalized dissolution rate, k'_T ($\text{g}\cdot\text{m}^{-2}\cdot\text{d}^{-1}$) represents the apparent normalized dissolution rate at $-\log(\text{H}_3\text{O}^+) = 0$. Here, k'_T is independent of the leachate acidity but temperature dependent. The term k'' is the normalized dissolution rate constant independent of temperature ($\text{g}\cdot\text{m}^{-2}\cdot\text{d}^{-1}$).

The n parameter corresponds to the partial order related to the proton activity, (H_3O^+) , and $\gamma_{\text{H}_3\text{O}^+}$ corresponds to the proton activity coefficient. It was usually determined from the variation of $\log(R_L)$ versus $\log(\text{H}_3\text{O}^+)$. In this study, $\gamma_{\text{H}_3\text{O}^+}$ values were calculated according to the SIT or Pitzer models, depending on the ionic strength considered.⁴⁰ The obtained partial orders related to protons, n (and to hydroxide ions in basic media), were generally found between 0 and 1 for several oxide-based materials (Table 2) suggesting the presence of surface reactions controlling the material dissolution.

Table 2. Partial Order Related to the Proton Activity and Activation Energy Obtained during the Dissolution of Several Oxide-Based Materials

mineral/material	partial order n	ref	E_A ($\text{kJ}\cdot\text{mol}^{-1}$)	ref
CeO ₂	0.63 ± 0.05	12	36 ± 5^a	12
Ce _{0.91} Nd _{0.09} O _{1.955}	1.10 ± 0.10	12	37 ± 5^a	12
ThO ₂	0.26 ± 0.05	8		
	0.41 ± 0.05	7	20 ± 3	7
Th _{0.81} Ce _{0.19} O ₂	0.50 ± 0.01	13	57 ± 6	13
UO ₂	0.91 ± 0.09	8		
	0.53	42	35 ± 3	43
Th _{0.63} U _{0.37} O ₂	0.30 ± 0.01	8		
	0.55 ± 0.10	7	33 ± 4	7
Th _{0.87} Pu _{0.13} O ₂	0.50 ± 0.06	9	ND ^b	
U _{0.75} Pu _{0.25} O ₂	1.7	44	10–32	44

^aUncertainty evaluated from the data reported in ref 12 and that determined on the Th_{1-x}Ce_xO₂ series.¹³ ^bNot determined.

In eq 3, E_A corresponds to the apparent activation energy of the mineral dissolution ($\text{kJ}\cdot\text{mol}^{-1}$). It was usually determined from the variation of $\ln(R_L)$ versus the reciprocal temperature. Due to the formation of adsorbed species onto the surface of leached materials, such E_A values were usually found to be significantly lower than the energy of the formation of chemical bonds²⁷ (Table 2). In this way, most of the available theories indicated that the dissolution reaction was controlled by the decomposition of an activated complex⁴¹ involving the adsorption of aqueous species onto the surface, reaction of these adsorbed species among themselves or with atoms of the surface, and finally desorption of the product species formed at the solid/liquid interface. The last step was usually slower and therefore controlled the overall rate of the sample dissolution.⁴¹

3. RESULTS AND DISCUSSION

3.1. General Trend of the Ce_{1-x}Ln_xO_{2-x/2} Dissolution.

The evolution of the normalized weight loss determined from the concentration of cerium and trivalent lanthanide (e.g., neodymium) in solution is reported in 4 M HNO₃ for Ce_{0.90}Nd_{0.10}O_{1.95} and Ce_{0.24}Nd_{0.76}O_{1.62}, respectively, at $T = 60$ and 2 °C (Figure 1).

While eq 2, describing the theoretical behavior of the dissolution process is supposed to lead to a linear evolution of

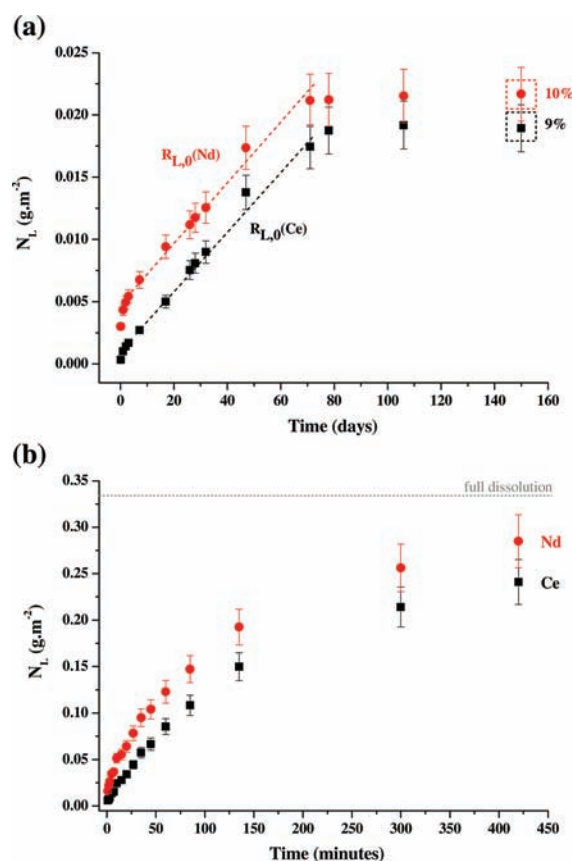


Figure 1. Evolution of the normalized weight loss determined during the dissolution in 4 M HNO₃ of Ce_{0.90}Nd_{0.10}O_{1.95} at $T = 60$ °C (a) and of Ce_{0.24}Nd_{0.76}O_{1.62} at $T = 2$ °C (b).

the normalized leaching, the results obtained during this study generally exhibit three distinct parts:

- During the initiation of the dissolution reaction, the release associated with the trivalent lanthanide was found to be systematically higher than that of cerium. Two hypotheses can be proposed to explain this initial incongruent behavior. The first one deals with the eventual existence of a Ln³⁺-enriched secondary phase at the surface of the sample which is expected to dissolve faster than the bulk material. Also, the segregation of trivalent lanthanide from cerium(IV) during the heat treatment process was already observed^{45–47} and generally led to a Ln³⁺-enrichment of a few nanometres of the surface layer. Moreover, such a layer was evidenced elsewhere through X-ray reflectivity (XRR) and grazing incidence X-ray diffraction (GI-XRD), performed either on raw and altered samples.⁴⁸ The preferential release of trivalent lanthanides could then correspond to the dissolution of such layer before that of the bulk material. Also, for the polyphase samples prepared for $x_{\text{Nd}} > 0.73$, the preferential release of neodymium arises from the rapid dissolution of the Nd₂O₃ secondary phase which was reported to be widely faster than that of CeO₂.⁴⁹ Nevertheless, it is important to underline that, whatever the sample considered, the eventual artifacts linked to the pulse observed in the Ln^{III} release could be avoided by performing a washing step prior to the beginning of the dissolution test. Surface layers of few nanometres could also be avoided using soft

ablation by plasma induction: for example, glow discharge can usually remove top surface layers without any effect on the bulk material.⁵⁰

- After the elimination of the more soluble fraction of the solid, the release of the trivalent lanthanide slows down. The normalized dissolution rate then became close to that of cerium. The dissolution can thus be considered as stoichiometric and congruent on that part of the graph which led to the determination of the normalized dissolution rate $R_{L,0}$.
- Finally, in some cases, a strong decrease of the normalized dissolution rate was observed for long leaching times. This behavior was usually linked to the apparition of thermodynamics-driven phenomena when approaching the saturation of solution, such as the formation of gelatinous/amorphous layers and/or precipitation of neoformed phases. The associated normalized dissolution rate determined in such conditions is usually noted $R_{L,v}$ and will not be discussed therein.

3.2. Influence of Composition. The influence of the lanthanide incorporation rate in the CeO_2 matrix on the chemical durability was first evaluated considering the $\text{Ce}_{1-x}\text{Nd}_x\text{O}_{2-x/2}$ series. Dissolution tests were then undertaken in 4 M HNO_3 at $T = 60^\circ\text{C}$ for several samples with x ranging from 0.10 to 0.59 (Figure 2). As shown by the variation of the

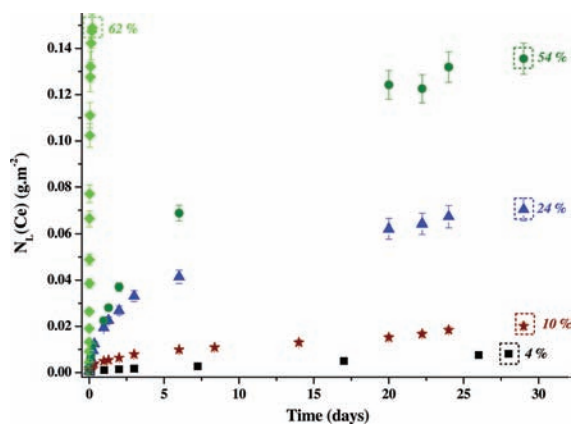


Figure 2. Evolution of the normalized weight loss $N_L(\text{Ce})$ determined during the dissolution of $\text{Ce}_{1-x}\text{Nd}_x\text{O}_{2-x/2}$ solid solutions in 4 M HNO_3 at $T = 60^\circ\text{C}$: $x_{\text{Nd}} = 0.10$ (square); 0.20 (star); 0.29 (triangle); 0.34 (circle); and 0.59 (diamond). The percentage of dissolved solid is indicated for the last point of each series.

normalized weight loss calculated from the cerium amount in solution, the normalized dissolution rate appears to be strongly correlated to the chemical composition. Indeed, only 4% of the solid was dissolved after 4 weeks for $x_{\text{Nd}} = 0.10$ while it reached 54% for $x_{\text{Nd}} = 0.34$. Moreover, the complete dissolution was achieved within only few hours when increasing the neodymium incorporation rate up to $x_{\text{Nd}} = 0.59$.

This strong influence was also emphasized by the values of the normalized dissolution rates determined in 4 M HNO_3 ($T = 60^\circ\text{C}$) (Table 3) which were increased by 7 orders of magnitude between pure CeO_2 ($R_{L,0}(\text{Ce}) = 3.5 \times 10^{-5} \text{ g}\cdot\text{m}^{-2}\cdot\text{d}^{-1}$) and polyphase $\text{Ce}_{0.24}\text{Nd}_{0.76}\text{O}_{1.62}$ ($R_{L,0}(\text{Ce}) = 200 \text{ g}\cdot\text{m}^{-2}\cdot\text{d}^{-1}$). Such an effect could probably be associated to a weakening of the crystal structure with the incorporation of trivalent elements, as also suggested by the direct comparison

Table 3. Normalized Dissolution Rates Determined during the Dissolution of $\text{Ce}_{1-x}\text{Nd}_x\text{O}_{2-x/2}$ Solid Solutions in 4 M HNO_3 at $T = 60^\circ\text{C}$ and Associated Ratios of Congruence (r)

x_{Nd}	$R_{L,0}(\text{Ce})$ ($\text{g}\cdot\text{m}^{-2}\cdot\text{d}^{-1}$)	$R_{L,0}(\text{Nd})$ ($\text{g}\cdot\text{m}^{-2}\cdot\text{d}^{-1}$)	$r = R_{L,0}(\text{Nd})/R_{L,0}(\text{Ce})$
0.00	$(3.5 \pm 0.4) \times 10^{-5}$		
0.10	$(2.5 \pm 0.3) \times 10^{-4}$	$(2.5 \pm 0.3) \times 10^{-4}$	1.00
0.20	$(6.0 \pm 0.6) \times 10^{-4}$	$(5.8 \pm 0.6) \times 10^{-4}$	0.97
0.24	$(1.9 \pm 0.2) \times 10^{-3}$	$(2.0 \pm 0.2) \times 10^{-3}$	1.05
0.29	$(7.1 \pm 0.7) \times 10^{-3}$	$(7.4 \pm 0.7) \times 10^{-3}$	1.04
0.34	$(1.5 \pm 0.2) \times 10^{-2}$	$(1.9 \pm 0.2) \times 10^{-2}$	1.27
0.39	$(3.4 \pm 0.3) \times 10^{-2}$	$(3.6 \pm 0.4) \times 10^{-2}$	1.06
0.42	$(8.6 \pm 0.9) \times 10^{-2}$	$(1.1 \pm 0.1) \times 10^{-1}$	1.28
0.48	$(4.1 \pm 0.4) \times 10^{-1}$	$(4.4 \pm 0.4) \times 10^{-1}$	1.08
0.59	3.6 ± 0.4	4.0 ± 0.4	1.11
0.68	$(6.6 \pm 0.7) \times 10^1$	$(7.4 \pm 0.7) \times 10^1$	1.12
0.73	$(1.5 \pm 0.2) \times 10^2$	$(1.7 \pm 0.2) \times 10^2$	1.14
0.77	$(2.0 \pm 0.2) \times 10^2$	$(2.2 \pm 0.2) \times 10^2$	1.02
0.79 ^a		$(6 \pm 3) \times 10^2$	
0.90 ^a		$(1.5 \pm 0.8) \times 10^3$	
0.97 ^a		$(8.5 \pm 4) \times 10^3$	

^aNormalized dissolution rates evaluated from the time required to reach the full sample dissolution.

of the calculated reticular energies of CeO_2 ($10\,200 \text{ kJ}\cdot\text{mol}^{-1}$) and Ce_2O_3 ($6200 \text{ kJ}\cdot\text{mol}^{-1}$) in the fluorite structure.⁵¹ Also, the normalized dissolution rates determined from the neodymium concentration in solution were systematically close to $R_{L,0}(\text{Ce})$ values with typically $0.9 < r = R_{L,0}(\text{Nd})/R_{L,0}(\text{Ce}) < 1.3$. These results thus confirmed that the dissolution reaction remained strictly stoichiometric and congruent once the Ln^{3+} -enriched phases and/or nanolayer present at the extreme surface was fully eliminated: in these conditions, both cerium and neodymium can be considered as tracers of the dissolution reaction.

Moreover, as it was stated before for other fluorite-type mixed dioxides,^{8,11} the variation of $\log(R_{L,0})$ was found to exhibit a linear trend versus x (Figure 3a). The associated slope was found to be about 9 which corresponds to an increase of the normalized dissolution rate by 1 order of magnitude for every 11% of neodymium incorporated.

Such a value could be put in parallel to that obtained when studying the effect of uranium(IV) incorporation in the ThO_2 matrix, which is widely reported to exhibit a very high chemical durability in nitric media, comparable with that of CeO_2 . In such conditions, the dissolution of $\text{Th}_{1-x}\text{U}_x\text{O}_2$ dioxides is not promoted by structural defects but by the oxidation of U(IV) into UO_2^{2+} molecular ion.^{7,8,42,43} Nevertheless, if one consider similar operating conditions than that used in this work, the variation of $\log R_{L,0}(\text{Th})$ versus x_{U} only presented a slope close to 5. Such difference may be correlated to the presence of oxygen vacancies in the whole solid while the oxidation of tetravalent uranium only occurs at the very extreme surface of the material (solid/solution interface) in the case of $\text{Th}_{1-x}\text{U}_x\text{O}_2$ mixed dioxides. In these conditions, once the first layer of atoms dissolved, $\text{Th}_{1-x}\text{U}_x\text{O}_2$ solid solutions again present an arrangement exempt of structural defects while cerium(IV)–lanthanide(III) mixed oxides keep exhibiting oxygen vacancies weakening the atoms located on cationic sites.

Furthermore, it is important to note that the linear variation of $\log(R_{L,0})$ versus x_{Nd} is maintained whatever the crystal structure of the mixed oxide considered. Indeed, both fluorite-

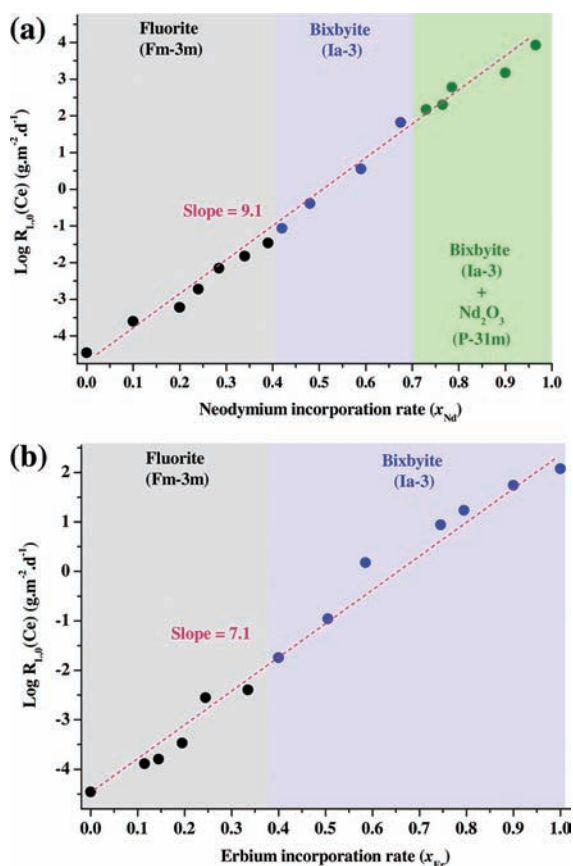


Figure 3. Variation of $\log R_{L,0}(\text{Ce})$ versus the trivalent lanthanide incorporation rate during the dissolution of $\text{Ce}_{1-x}\text{Ln}_x\text{O}_{2-x/2}$ solid solutions in 4 M HNO_3 at $T = 60^\circ\text{C}$: Ln = Nd (a) and Er (b).

and bixbyite-type compounds follow the same trend which could be explained by the close relation between both structures.^{52,53} More surprisingly, it is also the case for the polyphase compounds consisting in a bixbyite-type phase and additional neodymium sesquioxide. For these samples, the initial very rapid dissolution of Nd_2O_3 probably led to strong microstructural modifications in the solid which weakened its chemical durability. Nevertheless, such second-order effects^{12,13} are probably concealed by the rapid kinetics of the $\text{Ce}_{1-x}\text{Nd}_x\text{O}_{2-x/2}$ sample dissolution.

In order to point out the potential influence of the trivalent cation itself, a similar study was conducted on the $\text{Ce}_{1-x}\text{Er}_x\text{O}_{2-x/2}$ series (Figure 3b). In this case, the phase transition between fluorite- and bixbyite-type structures occurs for $x_{\text{Er}} \approx 0.39$ while the $Ia\bar{3}$ cubic superstructure is maintained up to $x_{\text{Er}} = 1$ ¹⁹ since it is usually the stable form for erbium sesquioxide (Er_2O_3).⁵⁴ Nevertheless, a similar behavior was stated compared to $\text{Ce}_{1-x}\text{Nd}_x\text{O}_{2-x/2}$ solid solutions. Indeed, the $\log R_{L,0}(\text{Ce})$ value increases linearly versus x_{Er} (slope close to 7), independently from the crystal structure considered. In this case, the slight difference noted in the slope compared to that determined for the $\text{Ce}_{1-x}\text{Nd}_x\text{O}_{2-x/2}$ series was assigned to the higher chemical durability measured in 4 M HNO_3 ($T = 2^\circ\text{C}$) for Er_2O_3 ($R_{L,0}(\text{Er}) \approx 0.2 \text{ g}\cdot\text{m}^{-2}\cdot\text{d}^{-1}$) compared to that of Nd_2O_3 ($R_{L,0}(\text{Nd}) \approx 70 \text{ g}\cdot\text{m}^{-2}\cdot\text{d}^{-1}$).

Finally, this study was extended to several solid solutions with general compositions $\text{Ce}_{0.7}\text{Ln}_{0.3}\text{O}_{1.85}$ and $\text{Ce}_{0.4}\text{Ln}_{0.6}\text{O}_{1.70}$ (Ln = La, Nd, Sm, Eu, Gd, Dy, Er and Yb) which were dissolved in 4 M HNO_3 at $T = 60^\circ\text{C}$ (Table 4). In order to get

Table 4. Normalized Dissolution Rates Determined during the Dissolution of $\text{Ce}_{0.7}\text{Ln}_{0.3}\text{O}_{1.85}$ and $\text{Ce}_{0.4}\text{Ln}_{0.6}\text{O}_{1.70}$ Solid Solutions in 4M HNO_3 at $T = 60^\circ\text{C}$ and Associated Congruence Ratios (r)

Ln ^{III}	$R_{L,0}(\text{Ce})$	$R_{L,0}(\text{Ln})$	$r = R_{L,0}(\text{Ln})/R_{L,0}(\text{Ce})$
$\text{Ce}_{0.7}\text{Ln}_{0.3}\text{O}_{1.85}$			
La	$(6.6 \pm 0.7) \times 10^{-3}$	$(8.5 \pm 0.9) \times 10^{-3}$	1.3
Nd	$(1.0 \pm 0.1) \times 10^{-2}$	$(1.0 \pm 0.1) \times 10^{-2}$	1.0
Sm	$(4.9 \pm 0.8) \times 10^{-3}$	$(6.4 \pm 0.7) \times 10^{-3}$	1.3
Gd	$(7.9 \pm 0.7) \times 10^{-3}$	$(9.2 \pm 0.9) \times 10^{-3}$	1.2
Dy	$(2.5 \pm 0.2) \times 10^{-3}$	$(3.1 \pm 0.3) \times 10^{-3}$	1.2
Er	$(1.6 \pm 0.2) \times 10^{-3}$	$(1.8 \pm 0.2) \times 10^{-3}$	1.1
Yb	$(3.1 \pm 0.3) \times 10^{-3}$	$(7.5 \pm 0.8) \times 10^{-3}$	2.4
$\text{Ce}_{0.4}\text{Ln}_{0.6}\text{O}_{1.70}$			
La	45 ± 5	50 ± 5	1.1
Nd	4.6 ± 0.5	5.1 ± 0.5	1.1
Sm	3.2 ± 0.3	3.5 ± 0.4	1.1
Eu	2.7 ± 0.3	3.1 ± 0.3	1.1
Gd	2.4 ± 0.2	2.4 ± 0.2	1.0
Dy	$(7.8 \pm 0.8) \times 10^{-1}$	$(7.8 \pm 0.8) \times 10^{-1}$	1.0
Er	2.3 ± 0.2	2.5 ± 0.2	1.1
Yb	$(2.9 \pm 0.3) \times 10^{-1}$	$(3.4 \pm 0.3) \times 10^{-1}$	1.2

an accurate comparison of the normalized dissolution rate, the precise composition of each sample was determined by X-EDS (see Table 1) then the corresponding $R_{L,0}$ value was corrected on the basis of the results obtained for the variation of $\log R_{L,0}$ versus x in the $\text{Ce}_{1-x}\text{Nd}_x\text{O}_{2-x/2}$ series, i.e.:

$$\log R_{L,0}(\text{Ce}) = 9.1x_{\text{Nd}} - 4.8 \quad (4)$$

Whatever the lanthanide element considered, the release of cations in the leachate remains congruent. Indeed, only the leaching of $\text{Ce}_{0.7}\text{Yb}_{0.3}\text{O}_{1.85}$ led to awkward r values that could be linked to the possible formation of (F + F)- or (F + C)-type polyphase compounds.^{19,55} Moreover, the general trend of the dissolution curves did not appear to be significantly modified along the lanthanide series (see Figure S1, Supporting Information). Despite the higher value obtained for lanthanum-based samples, which could be explained by their strong tendency to hydroxylation,^{56,57} the normalized dissolution only slightly decrease with the atomic weight of the rare earth element: it is of note that this effect is even more observable for the compounds with $x = 0.6$, probably due to the higher substitution rate considered.

Two hypothesis could be proposed to explain the decrease of $R_{L,0}(\text{Ce})$ along the lanthanide series:

- The first one deals with a modification of the cohesion energy of the fluorite-type unit cell with the incorporation of trivalent elements. Indeed, if the values corresponding to mixed oxides are not properly reported in the literature, that of pure end members revealed that the reticular energy of lanthanide sesquioxides varies from 12 450 $\text{kJ}\cdot\text{mol}^{-1}$ for La_2O_3 to 13 380 $\text{kJ}\cdot\text{mol}^{-1}$ for Yb_2O_3 .⁵⁸ On this basis, the higher cohesion energy related to heavy rare earth elements (HREE) oxides could be associated to the higher chemical durability of the HREE-doped CeO_2 samples.

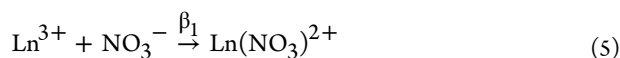
Table 5. Normalized Dissolution Rates Determined during the Dissolution of Ce_{1-x}Nd_xO_{2-x/2} Solid Solutions in 4 M HNO₃ at Various Temperatures^a

<i>x</i> _{Nd}	<i>R</i> _{L,0} (i) (g·m ⁻² ·d ⁻¹)				
	90 °C	75 °C	40 °C	25 °C	2 °C
0.00	(5.5 ± 0.6) × 10 ⁻⁵				
0.10	(1.6 ± 0.2) × 10 ⁻³ (2.0 ± 0.2) × 10 ⁻³	(8.2 ± 0.8) × 10 ⁻⁴ (8.2 ± 0.8) × 10 ⁻⁴			
0.20	(1.1 ± 0.1) × 10 ⁻² (5.0 ± 0.5) × 10 ⁻³				
0.24	(4.7 ± 0.5) × 10 ⁻² (4.6 ± 0.5) × 10 ⁻²				
0.29	(1.3 ± 0.1) × 10 ⁻¹ (1.4 ± 0.1) × 10 ⁻¹	(7.5 ± 0.8) × 10 ⁻² (9.6 ± 1.0) × 10 ⁻²	(6.8 ± 0.7) × 10 ⁻⁴ (9.3 ± 0.9) × 10 ⁻⁴	(4.1 ± 0.4) × 10 ⁻⁴ (3.7 ± 0.4) × 10 ⁻⁴	(1.7 ± 0.2) × 10 ⁻⁵ (3.3 ± 0.3) × 10 ⁻⁵
0.34	(1.7 ± 0.2) × 10 ⁻¹ (1.7 ± 0.2) × 10 ⁻¹				
0.39	2.3 ± 0.2 2.4 ± 0.2				
0.42	2.2 ± 0.2 2.5 ± 0.2	(4.6 ± 0.5) × 10 ⁻¹ (5.8 ± 0.6) × 10 ⁻¹	(3.7 ± 0.4) × 10 ⁻² (4.3 ± 0.4) × 10 ⁻²	(4.3 ± 0.4) × 10 ⁻³ (5.2 ± 0.5) × 10 ⁻³	
0.48	9.2 ± 0.2 10 ± 1				
0.59	54 ± 5 55 ± 6	10 ± 1 11 ± 1	1.0 ± 0.1 1.1 ± 0.1	(1.7 ± 0.2) × 10 ⁻¹ (1.8 ± 0.2) × 10 ⁻¹	(6.0 ± 0.6) × 10 ⁻³ (6.7 ± 0.6) × 10 ⁻³
0.68	820 ± 80 970 ± 90				
0.73	1000 ± 500 ^b				(2.1 ± 0.2) × 10 ⁻¹ (2.6 ± 0.3) × 10 ⁻¹
0.74					(6.8 ± 0.7) × 10 ⁻¹ (8.9 ± 0.9) × 10 ⁻¹
0.79			170 ± 20 210 ± 20	35 ± 4 45 ± 4	2.2 ± 0.2 3.3 ± 0.3
0.90					8.3 ± 0.8 12 ± 1
0.97					100 ± 10 170 ± 10
1					71 ± 7

^a*R*_{L,0}(Ce) values are gathered in normal text while *R*_{L,0}(Nd) appears in italics. The values obtained at *T* = 60 °C are gathered in Table 3.

^bNormalized dissolution rate evaluated from the time required to reach the full dissolution of the solid.

- The variation of the normalized dissolution rate could be also compared to that of the constant associated to the nitrate complexation along the lanthanide series through:



- Indeed, this latter shows higher values for light rare earth elements.^{59,60} As the complexing anions could play an important role during the dissolution process of fluorite-type oxides, like ThO₂,^{9,61–63} such variation of the β_1 constant could explain the higher normalized dissolution rate determined for samples incorporating light rare earth elements such as lanthanum.

3.3. Influence of Temperature. As expected from eq 3, the temperature was found to modify significantly the dissolution kinetics, the normalized dissolution rates being widely increased when raising the temperature. As an example, the *R*_{L,0}(Ce) value determined during the dissolution of Ce_{0.71}Nd_{0.29}O_{1.855} in 4 M HNO₃ was found to increase from 10⁻⁵ g·m⁻²·d⁻¹ at *T* = 2 °C to about 10⁻¹ g·m⁻²·d⁻¹ at *T* = 90 °C, i.e. by 4 orders of magnitude (Table 5). Nevertheless, the general trends of the dissolution curves did not appear to be strongly affected by the increase of temperature (see Supporting Information Figure S2): indeed, the dissolution

was always found to be congruent while two distinct steps were identified. The first one was related to pure kinetic control of dissolution while the second one showed a decrease of the normalized dissolution rate, probably due to the establishment of diffusion phenomena linked to the formation of amorphous and/or crystallized surface phases.³⁰ In these conditions, the temperature did not appear to modify significantly the reaction mechanism for the operating conditions considered, whatever the chosen composition. Moreover, the influence of the neodymium incorporation rate on the dissolution of Ce_{1-x}Nd_xO_{2-x/2} solid solutions was found to be constant between 2 and 90 °C (Figure 4). Indeed, in this range of temperature, the variation of log *R*_{L,0}(Ce) versus *x*_{Nd} always followed a linear trend with a slope ranging between 8.2 and 10.5 (average value of 9.1).

Also, from all the data gathered in Tables 3 and 5, the variation of ln *R*_{L,0}(Ce) versus the reciprocal temperature was plotted for several compositions of Ce_{1-x}Nd_xO_{2-x/2} solid solutions and allowed the determination of activation energies (*E*_A) and pre-exponential factors (*k*⁰) related to the reaction of dissolution (Figure 5, Table 6).

For all the systems considered, the linear variation of ln *R*_{L,0}(Ce) versus 1/*T* confirmed the constancy of *E*_A on the temperature range considered. Moreover, the activation energy

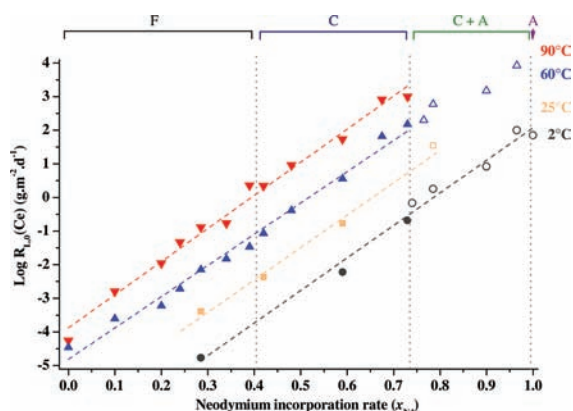


Figure 4. Variation of $\log R_{L,0}(\text{Ce})$ versus the neodymium incorporation rate (x_{Nd}) for several temperatures (4 M HNO_3): 2 (dark gray), 25 (orange), 60 (blue), and 90 °C (red). Full symbols correspond to single-phase samples while open ones stand for polyphase compounds and for pure Nd_2O_3 . For this latter, the value of $\log R_{L,0}(\text{Nd})$ is supplied for comparison purpose.

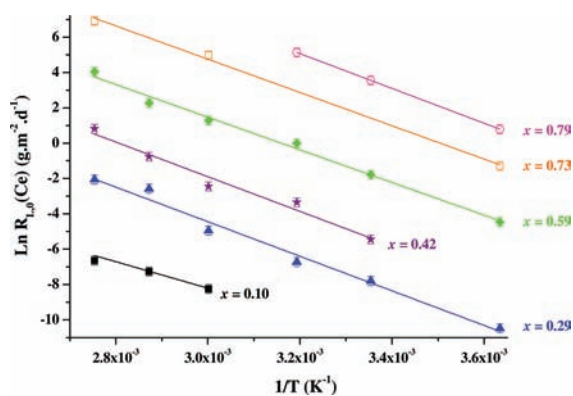


Figure 5. Variation of $\ln R_{L,0}(\text{Ce})$ versus the reciprocal temperature for several compositions of $\text{Ce}_{1-x}\text{Nd}_x\text{O}_{2-x/2}$ solid solutions (4 M HNO_3).

was always found to be close to $80 \text{ kJ}\cdot\text{mol}^{-1}$ for $0.29 \leq x_{\text{Nd}} \leq 0.80$: such a value excluded the control of the dissolution through diffusion phenomena⁶⁴ and indicated more likely that the dissolution occurred through surface-controlled mechanisms involving the formation of complexes on active surface sites.²⁷ Also, this value did not appear to be dependent on the nature of the trivalent lanthanide cation incorporated in the CeO_2 structure since activation energies close to $80 \text{ kJ}\cdot\text{mol}^{-1}$ were also determined during the dissolution of $\text{Ce}_{1-x}\text{Er}_x\text{O}_{2-x/2}$ solid solutions with $x_{\text{Er}} = 0.34$ and 0.80 . On this basis, both temperature and composition appeared to be independent parameters regarding to the dissolution kinetics.

These values were then compared with that previously determined for the dissolution of CeO_2 in oxidative media. Towards this purpose, the data collected in the same operating conditions (about $40 \text{ kJ}\cdot\text{mol}^{-1}$ in 10^{-1} –6 M HNO_3)¹² was adopted as reference since other activation energies reported in the literature exhibited strong variations and high values (up to $100 \text{ kJ}\cdot\text{mol}^{-1}$)⁶⁵ that seemed off the range usually obtained for ceramic materials (see for example the values obtained for ThO_2). The values obtained therein during the dissolution of $\text{Ce}_{1-x}\text{Nd}_x\text{O}_{2-x/2}$ and $\text{Ce}_{1-x}\text{Er}_x\text{O}_{2-x/2}$ solid solutions revealed a strong increase in the activation energy between the pure CeO_2 and the Ln^{III} -bearing compounds. As the lanthanide weight

Table 6. Activation Energies (E_A) and Associated Pre-exponential Factors (k'') Determined during the Dissolution of $\text{Ce}_{1-x}\text{Nd}_x\text{O}_{2-x/2}$ and $\text{Ce}_{1-x}\text{Er}_x\text{O}_{2-x/2}$ Solid Solutions in Nitric Media

sample	leaching media	E_A ($\text{kJ}\cdot\text{mol}^{-1}$)	k'' ($\text{g}\cdot\text{m}^{-2}\cdot\text{d}^{-1}$)	ref
CeO_2	7 M HNO_3	102 ± 9		65
CeO_2	0.1–6 M HNO_3	36 ± 5^a		12
ThO_2	10^{-2} M HNO_3 + 0.1 M KNO_3	20 ± 3		7
$\text{Th}_{0.81}\text{Ce}_{0.19}\text{O}_2$	2 M HNO_3	57 ± 6	4.5×10^3	13
$\text{Ce}_{0.91}\text{Nd}_{0.09}\text{O}_{1.955}$	0.1–6 M HNO_3	37 ± 5^a		12
$\text{Ce}_{0.90}\text{Nd}_{0.10}\text{O}_{1.95}$	4 M HNO_3	62 ± 8	1.7×10^6	this study
$\text{Ce}_{0.715}\text{Nd}_{0.285}\text{O}_{1.86}$		86 ± 3	3.3×10^{11}	
$\text{Ce}_{0.575}\text{Nd}_{0.425}\text{O}_{1.79}$		81 ± 5	7.3×10^{11}	
$\text{Ce}_{0.41}\text{Nd}_{0.59}\text{O}_{1.705}$		84 ± 5	2.6×10^{13}	
$\text{Ce}_{0.27}\text{Nd}_{0.73}\text{O}_{1.635}$		81 ± 8	6.0×10^{14}	
$\text{Ce}_{0.215}\text{Nd}_{0.785}\text{O}_{1.61}$		82 ± 8	4.0×10^{14}	
$\text{Ce}_{0.67}\text{Er}_{0.33}\text{O}_{1.83}$		82 ± 5	3.8×10^{10}	
$\text{Ce}_{0.21}\text{Er}_{0.79}\text{O}_{1.60}$		74 ± 3	5.5×10^{15}	

^aUncertainty evaluated from the data reported in ref 12 and that determined on the $\text{Th}_{1-x}\text{Ce}_x\text{O}_2$ series.¹³

loading did not modify significantly the E_A value beyond $x_{\text{Ln}} = 0.1$, it appeared that the incorporation of a trivalent cation, and the subsequent formation of oxygen vacancies, acts as a threshold effect which strongly enhanced the dependence of the normalized dissolution rate with the temperature. Such an effect could probably be associated to the weakening of the crystal structure with the incorporation of trivalent elements.

3.4. Influence of Acidity. As the dissolution rate of a ceramic material generally depends on the concentration of reactive species in the leaching media, such as H_3O^+ (see eq 3), the influence of the acidity was also considered in this study. In this aim, two samples ($\text{Ce}_{0.71}\text{Nd}_{0.29}\text{O}_{1.855}$ and $\text{Ce}_{0.41}\text{Nd}_{0.59}\text{O}_{1.71}$) were altered in 10^{-4} to 4 M HNO_3 . In order to allow the determination of the normalized dissolution rates for the lower acidities considered in a reasonable experiment time, the temperature was raised to 90 °C. The normalized dissolution rates determined from the release of cerium in the solution are gathered in Table 7 along with the activity of H_3O^+ , calculated from Pitzer or SIT models,⁴⁰ depending on the HNO_3 concentrations considered.

As it was expected, the normalized dissolution rate of both $\text{Ce}_{1-x}\text{Ln}_x\text{O}_{2-x/2}$ solid solutions was found to increase strongly with (H_3O^+), since the $R_{L,0}(\text{Ce})$ value was generally increased by a factor 5 when raising the acid concentration by 1 order of magnitude. Nevertheless, for the lower acidities considered (typically for $\text{pH} \geq 2$), the determination of the normalized dissolution rates was affected, or even precluded, by the precipitation of neoformed phases associated to the saturation of the leaching solution. Even if the identification of such phases remains hardly achievable, one can consider that it was probably constituted either by hydroxide or hydrated oxide phases, as suggested by the low solubility constants of $\text{Ln}(\text{OH})_3$ ($-28 < \log K_s^0 < -19$)⁵⁷ and especially $\text{Ce}(\text{OH})_4$ ($\log K_s^0 = -50$).⁶⁶

On this basis, the determination of the partial order related to the proton concentration in solution, n , was only conducted

Table 7. Normalized Dissolution Rates Determined during the Dissolution of $Ce_{1-x}Nd_xO_{2-x/2}$ Solid Solutions in Nitric Media ($T = 90\text{ }^\circ\text{C}$)

leaching media	(H_3O^+)		$R_{L,0}$ ($g\cdot m^{-2}\cdot d^{-1}$)	
			$Ce_{0.71}Nd_{0.29}O_{1.855}$	$Ce_{0.41}Nd_{0.59}O_{1.705}$
04 M HNO_3	3.82	Ce	$(1.3 \pm 0.1) \times 10^{-1}$	$(5.4 \pm 0.5) \times 10^1$
		Nd	$(1.4 \pm 0.1) \times 10^{-1}$	$(5.5 \pm 0.5) \times 10^1$
1 M HNO_3	0.74	Ce	$(5.3 \pm 0.5) \times 10^{-2}$	5.4 ± 0.5
		Nd	$(6.3 \pm 0.6) \times 10^{-2}$	$(1.1 \pm 0.1) \times 10^1$
0.1 M HNO_3	8.0×10^{-2}	Ce	$(7.3 \pm 0.7) \times 10^{-3}$	$(3.8 \pm 0.4) \times 10^{-1}$
		Nd	$(8.1 \pm 0.7) \times 10^{-3}$	3.4 ± 0.3
10^{-2} M $HNO_3 + 0.1$ M KNO_3	8.0×10^{-3}	Ce	$(1.7 \pm 0.2) \times 10^{-3}$	$(7.3 \pm 3) \times 10^{-2}$
		Nd	$(1.7 \pm 0.2) \times 10^{-3}$	$(1.6 \pm 0.8) \times 10^{-1}$
10^{-4} M $HNO_3 + 0.1$ M KNO_3	8×10^{-5}	Ce	$(2.4 \pm 1.2) \times 10^{-4}$	$(1.0 \pm 0.5) \times 10^{-2}$
		Nd	$(2.0 \pm 1.0) \times 10^{-4}$	$(9.0 \pm 4.5) \times 10^{-3}$

between 10^{-2} and 4 M to avoid any bias due to saturation phenomena. For the two compositions considered, the variation of $\log R_{L,0}(Ce)$ followed a linear trend versus $-\log(H_3O^+)$ (Figure 6), leading to partial orders close to 0.7.

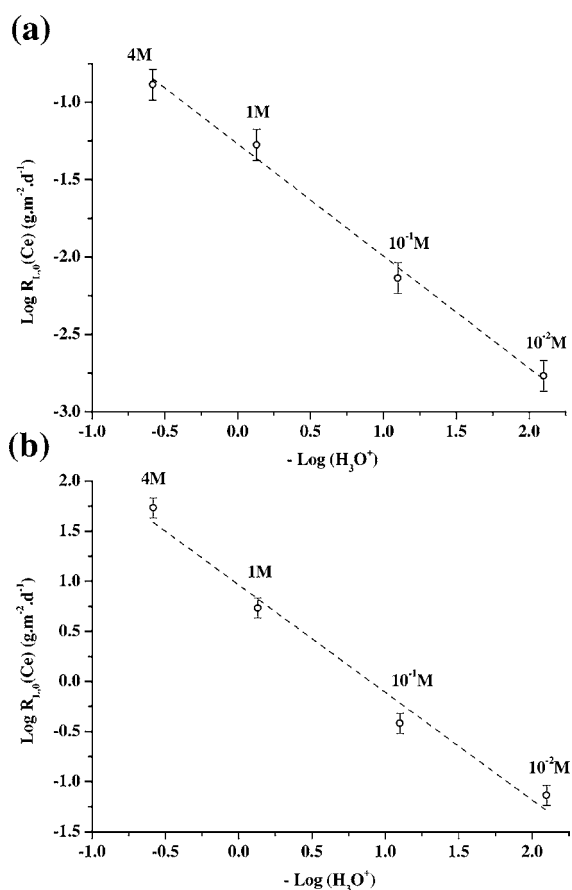


Figure 6. Variation of $\log R_{L,0}(Ce)$ versus $-\log(H_3O^+)$ during the dissolution of $Ce_{0.71}Nd_{0.29}O_{1.855}$ (a) and $Ce_{0.41}Nd_{0.59}O_{1.705}$ (b) solid solutions in HNO_3 ($T = 90\text{ }^\circ\text{C}$).

Such values appear in very good agreement with that previously reported in the literature for CeO_2 or $Ce_{0.91}Nd_{0.09}O_{1.955}$.¹² Conversely, they appeared rather higher than that determined for $Th_{1-x}Ce_xO_2$ solid solutions¹³ which could be correlated to the weakening of the solid induced by the presence of oxygen vacancies or to a modification of the amount of available reactive surface sites. Also, as the activation energies

determined in the previous section, they accounted for the existence of surface reactions involving H_3O^+ ions and controlling the kinetics of the dissolution process.

Finally, in order to verify that the influence of acidity remains constant on the whole composition range of $Ce_{1-x}Ln_xO_{2-x/2}$ solid solutions, five Nd-doped samples were altered in 0.1 M HNO_3 at $T = 90\text{ }^\circ\text{C}$. As it was first observed in 4 M HNO_3 (see section 3.2), the variation of the logarithm of the normalized dissolution rate versus the substitution rate x_{Nd} followed a linear trend (Figure 7). Moreover, the slope obtained in these

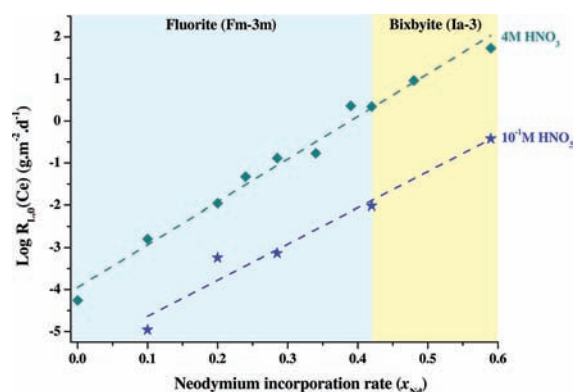


Figure 7. Variation of $\log R_{L,0}(Ce)$ versus the neodymium incorporation rate (x_{Nd}) during the dissolution of $Ce_{1-x}Nd_xO_{2-x/2}$ solid solutions in 4 M HNO_3 (diamond) and 10^{-1} M HNO_3 (star).

operating conditions (8.7) appeared close to that determined in 4 M HNO_3 , thus indicating that the effect of the acidity was independent of the chemical composition of the sample.

3.5. Influence of Inorganic Ligand. In order to complete the previous study concerning the effect of the acidity on the chemical durability of $Ce_{1-x}Ln_xO_{2-x/2}$ solid solutions, several dissolution tests were conducted in hydrochloric and sulphuric acids on $Ce_{0.4}Ln_{0.6}O_{1.7}$ samples. Whatever the medium considered, the general trend already described in nitric solutions was kept and the values of $R_{L,0}(Ce)$ obtained for a same compound remained close (Table 8), leading to a decrease of the normalized dissolution rate of the $Ce_{1-x}Ln_xO_{2-x/2}$ samples along the lanthanides series. Such observation indicates that the complexing anions only weakly impacted the dissolution kinetics. Indeed, only the $R_L(Ce)$ values measured for La-bearing samples appeared significantly different which could be associated to the higher complexation constants reported for lanthanum both in hydrochloric, nitric,

Table 8. Normalized Dissolution Rates Determined during the Dissolution of $Ce_{0.4}Ln_{0.6}O_{1.7}$ Solid Solutions at $T = 60\text{ }^{\circ}\text{C}$

Ln ^{III}	4 M HCl		4 M H ₂ SO ₄		4 M HNO ₃	
	$R_{L,0}(\text{Ce})$	$R_{L,0}(\text{Ln})$	$R_{L,0}(\text{Ce})$	$R_{L,0}(\text{Ln})$	$R_{L,0}(\text{Ce})$	$R_{L,0}(\text{Ln})$
La	140 ± 14	78 ± 8	63 ± 6	43 ± 4	45 ± 4	50 ± 5
Nd	10 ± 1.0	11 ± 1.1	3.2 ± 0.3	4.2 ± 0.4	4.6 ± 0.5	5.1 ± 0.5
Sm	2.5 ± 0.3	2.8 ± 0.3	1.7 ± 0.1	1.8 ± 0.1	3.2 ± 0.3	3.5 ± 0.3
Eu	1.4 ± 0.1	1.4 ± 0.1	1.4 ± 0.1	1.5 ± 0.1	2.7 ± 0.3	3.1 ± 0.3
Gd	1.3 ± 0.1	1.4 ± 0.1	1.2 ± 0.1	1.4 ± 0.1	2.4 ± 0.2	2.4 ± 0.2
Dy	0.78 ± 0.08	0.69 ± 0.07	0.65 ± 0.07	0.61 ± 0.06	0.78 ± 0.08	0.78 ± 0.08
Er	1.9 ± 0.1	1.2 ± 0.1	0.33 ± 0.03	0.19 ± 0.2	2.3 ± 0.2	2.5 ± 0.2
Yb	0.43 ± 0.04	0.47 ± 0.05	0.24 ± 0.02	0.29 ± 0.03	0.29 ± 0.03	0.34 ± 0.03

and sulphuric media.^{59,60} Such an observation appears in contradiction with the results reported by Hubert et al. during the dissolution of ThO₂ since they showed an increase of the dissolution rate by a factor of 8 between sulphuric and hydrochloric media.⁹ This difference could be assigned to the higher chemical durability of thorium oxide compared to Ce_{0.4}Ln_{0.6}O_{1.7} solid solutions (i.e., over 5 orders of magnitude). Also, as the incorporation of trivalent elements in the fluorite-type matrix constitutes the predominant parameter decreasing the chemical durability of the Ce_{1-x}Ln_xO_{2-x/2} solid solutions, it could preclude the observation of differences between the different acidic media. Indeed, such a slight effect could be concealed by the rapid kinetics of dissolution observed for the series of samples studied.

4. CONCLUSION

The dissolution of Ce_{1-x}Ln_xO_{2-x/2} solid solutions revealed a strong dependence on the chemical composition, i.e. trivalent lanthanide incorporation rate (x), which was compared to that exhibited regarding to usual physicochemical parameters such as temperature, acidity, or complexing agents. A summary of these effects is schematized in Figure 8 and confirms that the

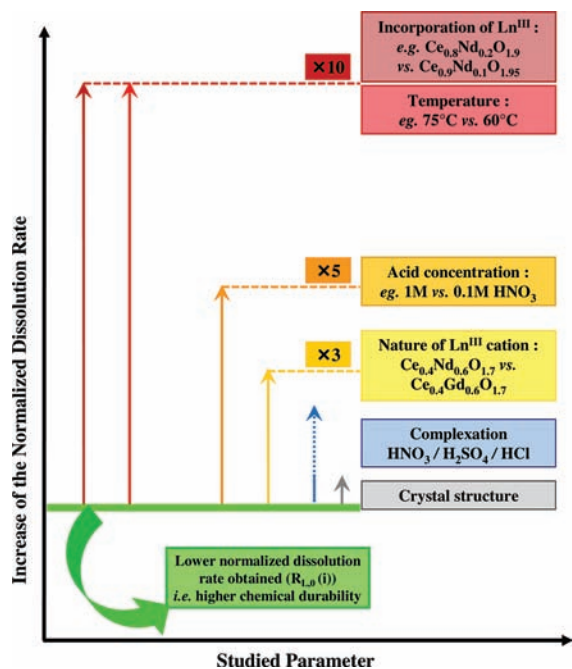


Figure 8. Relative influence of the various physicochemical parameters studied on the Ce_{1-x}Ln_xO_{2-x/2} solid solution normalized dissolution rate.

weakening of the crystal lattice due to oxygen vacancies, formed to counterbalance the charge deficit following Ln³⁺ incorporation, mainly impacts the dissolution kinetics. Indeed, the normalized dissolution rate was found to increase by almost 1 order of magnitude for each 10% of Ln³⁺ cations incorporated into the CeO₂ structure. From this point of view, it could be compared to the strong influence of redox reactions on the dissolution of several compounds such as the Th_{1-x}U_xO₂^{7,8} or Th_{1-x}Pu_xO₂ series.⁹ On the contrary, the nature of the trivalent cation considered appeared to weakly modify the kinetics, probably due to the close values of complexation constants regarding to nitrate ions.

The temperature appeared as the other first-order parameter to consider in order to foresee the behavior of Ce_{1-x}Ln_xO_{2-x/2} oxides during their dissolution. For example, the $R_{L,0}$ value was found to increase by 4 orders of magnitude between 2 and 90 °C. Also, the correlative determination of activation energy more likely indicated that the dissolution reaction is controlled by surface processes involving the formation of activated complexes.²⁷ The incorporation of aliovalent cations in the fluorite-type matrix of CeO₂ then did not appear to modify strongly the mechanisms of dissolution. A similar conclusion was made from the study of the influence of the acidity on the normalized dissolution rates. Indeed, the partial order related to the proton activity ($n \approx 0.7$) also argued for a surface-controlled reaction. Moreover, while the influence of acid concentration appeared to be moderate, that of complexing agent was not evidenced in this study, probably concealed by the prevailing effect of Ln³⁺ cation incorporation. The subsequent rapid kinetics can also probably explain that no differences were observed when modifying the crystal structure of the samples. Also, it would probably preclude the observation of any effect coming from microstructural modifications such as crystallization state, densification state, or grain size.¹²

In order to complete this work, further investigations are already under progress on sintered samples and aim particularly to fully characterize the surface phases present on the raw material as well as that precipitated in the back end of the initial dissolution step for the lowest acid concentrations. In the first case, the existence of Ln-enriched layers is supposed to induce a chemical gradient called interphase. In the second one, the deposition of a neoformed phase would be characterized by an interface which does not rely on any chemical gradient but more likely to two systems differing by their texture, structure, and/or chemical composition. In these conditions, TEM coupled with X-EDS, GD-OES, or XRR/GI-XRD measurements could allow sorting out and characterizing interfaces and interphases, which conditioned the reaction kinetics.

Also, similar multiparametric studies will be devoted to more complex systems: among them, those involving the joint influence of redox reactions and of aliovalent cations incorporation, such as the $U_{1-x}Ln_xO_{2-x/2}$ series, will be especially pointed out in order to progress in the understanding of nuclear spent fuel behavior during dissolution.

■ ASSOCIATED CONTENT

● Supporting Information

Evolution of $N_L(\text{Ce})$ during the dissolution of $\text{Ce}_{0.7}\text{Ln}_{0.3}\text{O}_{1.85}$ and $\text{Ce}_{0.4}\text{Nd}_{0.6}\text{O}_{1.70}$ in 4 M HNO_3 at $T = 60^\circ\text{C}$. Evolution of $N_L(\text{Ce})$ during the dissolution of $\text{Ce}_{0.71}\text{Nd}_{0.29}\text{O}_{1.86}$ and $\text{Ce}_{0.41}\text{Nd}_{0.59}\text{O}_{1.71}$ in 4 M HNO_3 at $T = 2, 40, 60,$ and 90°C . This material is available free of charge via the Internet at <http://pubs.acs.org/>.

■ AUTHOR INFORMATION

Corresponding Author

*Tel.: +33 4 66 33 92 08. Fax: +33 4 66 79 76 11. E-mail: nicolas.clavier@icsm.fr.

Notes

The authors declare no competing financial interest.

■ ACKNOWLEDGMENTS

The authors would like to thank the MATINEX French Research Group (*Innovative materials in extreme conditions*, CEA/CNRS/AREVA/EDF/French Universities) included in the PACEN Program for their subsequent financial support. This work also benefited from financial support of the French National Research Agency (ANR, project no. ANR-08-BLAN-0216) and from the CNRS Interdisciplinary Research Program MaProSu (Matériaux et Procédés de Remplacement/Substitution). Authors are also thankful to the referees of this paper for their precious advice concerning present and future works.

■ REFERENCES

- (1) Ichimiya, M.; Sagayama, Y. T. *Am. Nucl. Soc* **2004**, *90*, 46–47.
- (2) Hoffelner, W. *Chimia* **2005**, *59*, 977–982.
- (3) Tommasi, J.; Delpech, M.; Groullier, J. P.; Zaetta, A. *Nucl. Tech.* **1995**, *111*, 133–148.
- (4) Prieur, D.; Martin, P. M.; Jankowiak, A.; Gavilan, E.; Scheinost, A. C.; Herlet, N.; Dehaut, P.; Blanchart, P. *Inorg. Chem.* **2011**, *50*, 10437–12445.
- (5) Prieur, D.; Jankowiak, A.; Leorier, C.; Herlet, N.; Donnet, L.; Dehaut, P.; Maillard, C.; Laval, J. P.; Blanchart, P. *Powder Technol.* **2011**, *208*, 553–557.
- (6) Degueudre, C.; Bertsch, J.; Kuri, G.; Martin, M. *Energy Environ. Sci.* **2011**, *4*, 1651–1661.
- (7) Heisbourg, G.; Hubert, S.; Dacheux, N.; Ritt, J. *J. Nucl. Mater.* **2003**, *321*, 141–151.
- (8) Heisbourg, G.; Hubert, S.; Dacheux, N.; Purans, J. *J. Nucl. Mater.* **2004**, *335*, 5–13.
- (9) Hubert, S.; Heisbourg, G.; Dacheux, N.; Moisy, P. *Inorg. Chem.* **2008**, *47*, 2064–2073.
- (10) Hubert, S.; Barthelet, K.; Fourest, B.; Lagarde, G.; Dacheux, N.; Baglan, N. *J. Nucl. Mater.* **2001**, *297*, 206–213.
- (11) Hingant, N.; Clavier, N.; Dacheux, N.; Barre, N.; Hubert, S.; Obbade, S.; Taborda, F.; Abraham, F. *J. Nucl. Mater.* **2009**, *385*, 400–406.
- (12) Claparede, L.; Clavier, N.; Dacheux, N.; Moisy, P.; Podor, R.; Ravau, J. *Inorg. Chem.* **2011**, *50*, 9059–9072.
- (13) Claparede, L.; Clavier, N.; Dacheux, N.; Mesbah, A.; Martinez, J.; Szenknect, S.; Moisy, P. *Inorg. Chem.* **2011**, *50*, 11702–11714.
- (14) McBride, J. R.; Hass, K. C.; Poindexter, B. D.; Weber, W. H. *J. Appl. Phys.* **1994**, *76*, 2435–2441.
- (15) Minervini, L.; Zacate, M. O.; Grimes, R. W. *Solid State Ionics* **1999**, *116*, 339–349.
- (16) Guo, X.; Waser, R. *Prog. Mater. Sci.* **2006**, *51*, 151–210.
- (17) Ikuma, Y.; Shimada, E.; Okamura, N. *J. Am. Ceram. Soc.* **2005**, *88*, 419–423.
- (18) Hong, S. J.; Virkar, A. V. *J. Am. Ceram. Soc.* **1995**, *78*, 433–439.
- (19) Horlait, D.; Claparede, L.; Clavier, N.; Szenknect, S.; Dacheux, N.; Ravau, J.; Podor, R. *Inorg. Chem.* **2011**, *50*, 7150–7161.
- (20) Veilly, E.; du Fou de Kerdaniel, E.; Roques, J.; Dacheux, N.; Clavier, N. *Inorg. Chem.* **2008**, *47*, 10971–10979.
- (21) Wolcyrz, M.; Kepinski, L. *J. Solid State Chem.* **1992**, *99*, 409–413.
- (22) Dedov, N.; Bagryantsev, V. *Radiochemistry* **1996**, *38*, 24–26.
- (23) Cooper, M. J. *Acta Cryst. B* **1982**, *38*, 264–269.
- (24) Shannon, R. D. *Acta Cryst. A* **1976**, *32*, 751–767.
- (25) Dacheux, N.; Le Du, J. F.; Brandel, V.; Genet, M.; Decambox, P.; Moulin, C. *New J. Chem.* **1996**, *20*, 507–514.
- (26) Thomas, A. C.; Dacheux, N.; Le Coustumer, P.; Brandel, V.; Genet, M. *J. Nucl. Mater.* **2000**, *281*, 91–105.
- (27) Lasaga, A. C. *J. Geophys. Res.* **1989**, *89*, 4009–4025.
- (28) Dacheux, N.; du Fou de Kerdaniel, E.; Clavier, N.; Podor, R.; Aupiais, J.; Szenknect, S. *J. Nucl. Mater.* **2010**, *404*, 33–43.
- (29) Dacheux, N.; Clavier, N.; Ritt, J. *J. Nucl. Mater.* **2006**, *349*, 291–303.
- (30) Clavier, N.; du Fou de Kerdaniel, E.; Dacheux, N.; Le Coustumer, P.; Drot, R.; Ravau, J.; Simoni, E. *J. Nucl. Mater.* **2006**, *349*, 304–316.
- (31) Walther, J. V. *Am. J. Sci.* **1996**, *296*, 693–728.
- (32) Ganor, J.; Mogollon, J. L.; Lasaga, A. C. *Geochim. Cosmochim. Acta* **1995**, *59*, 1037–1052.
- (33) Pokrovsky, O. S.; Schott, J. *Geochim. Cosmochim. Acta* **2000**, *64*, 3313–3325.
- (34) Furrer, G.; Stumm, W. *Geochim. Cosmochim. Acta* **1991**, *55*, 2193–2201.
- (35) Chou, L.; Wollast, R. *The chemistry of weathering*; Kluwer: Dordrecht, Netherlands, 1985.
- (36) Chou, L.; Wollast, R. *Am. J. Sci.* **1985**, *258*, 963–993.
- (37) Furrer, G.; Stumm, W. *Geochim. Cosmochim. Acta* **1986**, *50*, 1847–1860.
- (38) Blum, A. E.; Lasaga, A. C. *Nature* **1988**, *331*, 431–433.
- (39) Robisson, A. C.; Dacheux, N.; Aupiais, J. *J. Nucl. Mater.* **2002**, *306*, 134–146.
- (40) Grenthe, I.; Puigdomenech, I. *Modelling in Aquatic Chemistry*; OECD Publications: Paris, France, 1997.
- (41) Eyring, H. *J. Chem. Phys.* **1935**, *3*, 107–115.
- (42) Bruno, J.; Casas, I.; Puigdomenech, I. *Geochim. Cosmochim. Acta* **1990**, *55*, 647–658.
- (43) De Pablo, J.; Casas, I.; Gimenez, J.; Molera, M.; Rovira, M.; Duro, L.; Bruno, J. *Geochim. Cosmochim. Acta* **1999**, *63*, 3097–3103.
- (44) Berger, P. *Etude du mécanisme de dissolution par oxydoréduction chimique et électrochimique des bioxydes d'actinides (UO_2 , NpO_2 , PuO_2 , AmO_2) en milieu aqueux acide*, PhD, no. 1988-PA06-6073, Université Paris VI, 1988.
- (45) Bellière, V.; Joost, G.; Stephan, O.; de Groot, F. M. F.; Weckhuysen, B. M. *J. Phys. Chem. B* **2006**, *110*, 9984–9990.
- (46) Luo, M. F.; Yan, Z. L.; Jin, L. Y.; He, M. *J. Phys. Chem. B* **2006**, *110*, 13068–13071.
- (47) Lei, Y.; Ito, Y.; Browning, N. D. *J. Am. Ceram. Soc.* **2002**, *85*, 2359–2363.
- (48) Szenknect, S.; Mesbah, A.; Horlait, D.; Clavier, N.; Dourdain, S.; Ravau, J.; Dacheux, N. *J. Phys. Chem.*, submitted for publication.
- (49) Girgin, I.; Yorukoglu, A. *Russ. J. Inorg. Chem.* **2010**, *55*, 646–654.
- (50) Le Coustumer, P.; Motelica-Heino, M.; Chapon, P.; Saint-Cyr, H. F.; Payling, R. *Surf. Interface Anal.* **2003**, *35*, 623–629.
- (51) Conesa, J. C. *Surf. Sci.* **1995**, *339*, 337–352.
- (52) Ou, D. R.; Mori, T.; Ye, F.; Zou, J.; Auchterlonie, G.; Drennan, J. *Phys. Rev. B* **2008**, *77*, 024108.

- (53) Andrievskaya, E. R.; Kornienko, O. A.; Sameljuk, A. V.; Sayir, A. *J. Eur. Ceram. Soc.* **2011**, *31*, 1277–1283.
- (54) Sibieude, F.; Foex, M. *J. Nucl. Mater.* **1975**, *56*, 229–238.
- (55) Mandal, B. P.; Grover, V.; Roy, M.; Tyagi, A. K. *J. Am. Ceram. Soc.* **2007**, *90*, 2961–2965.
- (56) Aizenshtein, M.; Shvareva, T. Y.; Navrotsky, A. *J. Am. Ceram. Soc.* **2010**, *93*, 4142–4147.
- (57) Diakonov, I. I.; Ragnarsdottir, K. V.; Tagirov, B. R. *Chem. Geol.* **1998**, *151*, 327–347.
- (58) *CRC Handbook of Chemistry and Physics*; Lide, D. R., Ed.; CRC Press: Boca Raton, FL, 2009.
- (59) Bonal, C.; Morel, J. P.; Morel-Desrosiers, N. *J. Chem. Soc. Farad. Trans.* **1998**, *94*, 1431–1436.
- (60) Ruas, A.; Moisy, P.; Simonin, J. P.; Bernard, O.; Dufreche, J. F.; Turq, P. *J. Phys. Chem. B* **2005**, *109*, 5243–5248.
- (61) Shying, M. E.; Florence, T. M.; Carswell, D. J. *J. Inorg. Nucl. Chem.* **1970**, *32*, 3493–3508.
- (62) Akabori, M.; Shiratori, T. *J. Nucl. Sci. Technol.* **1994**, *31*, 539–545.
- (63) Osthols, E.; Malmstrom, M. *Radiochim. Acta* **1995**, *68*, 113–119.
- (64) Tso, S. T.; Pask, J. A. *J. Am. Ceram. Soc.* **1982**, *65*, 360–362.
- (65) Joret, L.; Cote, G.; Bauer, D. *Hydrometallurgy* **1997**, *45*, 1–12.
- (66) Gopalan, S.; Singhal, S. C. *Scripta Mater.* **2000**, *42*, 993–996.